ANALYSIS OF STRESS CORROSION CRACKING OF HETEROGENEOUS WELDED JOINTS IN SIMULATED PRIMARY WATER ENVIRONMENT

UDC:620.194.2:621.791.052
Original scientific paper https://doi.org/10.46793/aeletters.2024.9.2.2

Marek Kudláč[1*], Mária Dománková[1], Peter Brziak[2], Alena Košinová[2], Matúš Gavalec[1], Katarína Bártová[1]

[1]Faculty of Materials Science and Technology in Trnava, Slovak University of Technology in Bratislava, J. Bottu 2781/25, 917 24 Trnava, Slovakia
[2]Research and Development Division of Welding Technologies and Equipment, Welding Research Institute, Račianska 1523, 831 02 Nové Mesto, Bratislava, Slovakia

Abstract:
The paper deals with the stress corrosion cracking of heterogeneous welded joints. The welded joints were made of austenitic base metal (AISI 321) and ferritic weld metal by arc welding. Two methods were used to analyze the stress corrosion cracking of samples of this type of welded joint. The first method was a slow strain rate test (SSRT) using a tabletop device at a temperature of 60°C with a graded strain rate for three specimens (10^{-5}, 10^{-6}, and 10^{-7} 1/s). The second method was exposure in a corrosion autoclave at a temperature of 270°C and pressure of 12.26 N/mm², while prestressing devices were used to achieve the prestressing at the level of yield strength and 3% plastic deformation. One specimen was bent to 60°. Boric acid solutions were used as the medium, which was supposed to simulate the environment of the primary circuit of nuclear power plants, a type of water-water energetic reactor. The surface and the presence of corrosion products, cracks, fractures, or pits on specimens were monitored using scanning electron microscopy, stereomicroscopy, confocal microscopy, and light microscopy. A gravimetric analysis was performed, as well, to determine the corrosion rate after exposure to the autoclave.

ARTICLE HISTORY
Received: 9 March 2024
Revised: 19 Apil 2024
Accepted: 20 May 2024
Published: 30 June 2024

KEYWORDS
Stress corrosion cracking, Welded joints, Autoclave, Corrosion, Primary water

1. INTRODUCTION

The phenomenon of stress corrosion cracking (SCC) is one of the most frequent degradation processes in the energy or chemical industry and causes significant complications in operations. The SCC includes three basic conditions: the presence of a corrosive environment, a material that is susceptible to cracking, and the presence of tensile stress. During the operation, there is a mechanical load (tension) of the material, where the combination of these three factors can lead to the initiation and growth of corrosion cracks and the formation of fractures. On the other hand, the material itself may already contain surface residual stresses, and fracture may not occur in the presence of external loading [1,2].

The primary circuit is the area where austenitic steels are used very often for their properties. However, SCCs were discovered at certain locations in the primary circuit during many inspections. SCC was often created by rupturing of oxide film which has duplex character – the first, external part is Fe-rich oxide with spinel structure type and inner side is Cr-rich oxide [3-6].

In the primary circuits of nuclear power plants with pressurized water reactors, austenitic steels such as AISI 304, 316, or 321 are usually used. It is AISI 321 that is stabilized with titanium to prevent the formation of $Cr_{23}C_6$ chromium carbides. Even though this was the stabilized stainless steel, there

*CONTACT: Marek Kudláč, e-mail: marek.kudlac@stuba.sk

are ways in which the corrosion process can be initiated (the presence of chlorides or deformation-induced martensite on the surface). In general, austenitic steels are susceptible to corrosion cracking in the environment of hot concentrated chloride solutions or by vapours polluted by chlorides [2,7].

Austenitic stainless steel and their weld joints have a significant problem with corrosion cracking in tests like a slow strain rate testing and in general with corrosion cracking in an environment containing chloride anions. Chloride ions penetrating the passivation layer and creating pitting are frequent SCC initiation sites in these steels [8-10]. In abnormal conditions in primary water, such as local area Cl^- reaching higher concentration or increasing dissolved oxygen concentration, the possibility of SCC of austenitic stainless steel structural materials, especially cold-worked materials, is greatly increased [11-13].

The welded joints form a separate part in connection with corrosion cracking. Those joints are the places where this type of degradation mechanism occurs to a greater extent. In the case of heterogeneous welded joints, when the base metal is austenitic steel, and the additional material is ferritic filler material, the galvanic (bimetallic) corrosion and its possible combination with stress corrosion cracking are also considered [14,15].

As was said before, the possibility of galvanic (bimetallic) corrosion in heterogeneous weld joints is common because the carbon steel weld metal has a lower nobility than the austenitic base metal. Many articles and monographs describe an increased susceptibility to this type of degradation damage. In addition to galvanic corrosion, hydrogen embrittlement is also a major problem. This can be formed again by an electrochemical reaction (depolarization) on the nobler side of the weld joint - the austenitic base material when hydrogen near the weld metal - base material interface penetrates the weld metal and causes hydrogen embrittlement. This problem commonly appears in the chemical or petroleum industry [16,17].

In this work, specimens of heterogeneous welded joints made of AISI 321 base metal and ferritic weld metal were observed, which were exposed to a boric acid solution (primary medium) while they were prestressed (in a corrosion autoclave) or pulled during the slow strain rate testing (SSRT). In both types of tests, a certain extreme parameter was used, namely, artificially added oxygen to the solution in a corrosion autoclave and an extreme type of stress at higher concentrations of boric acid.

2. MATERIALS AND METHODS

To assess the stress corrosion cracking, two tests were applied to the specimens, namely exposure in a corrosion autoclave, where the specimens were bent to selected prestress levels using the prestressing devices, and the slow strain rate test in a tabletop device, where in a chamber containing a boric acid solution, specimens were stretched at three different deformation rates. Two types of specimens were prepared: in the shape of a plate for exposure in the autoclave and in the shape of a tensile specimen for the slow strain rate test, while in both types of specimens, the weld metal was in the central part of these specimens. The base metal was austenitic stainless steel AISI 321 (chemical composition is shown in Table 1). The weld metal was created with ferritic filler metal-welding wire OK Tigrod 12.60 (chemical composition is shown in Table 2) with a diameter of 2.4 mm. The welded joints were executed by arc welding (TIG). The welding parameters were as follows: process 141, type of current =/-, voltage of 12 V, current of 140 A (100 A at the weld root), welding speed of 1.30 mm/s, heat input of 1.4 kJ/mm and shielding gas was Ar (99,99 %). The width of the root part of the weld was 6 mm.

Table 1. Chemical composition of AISI 321

Elements	**C**	**Si**	**Mn**	**Cr**
[wt. %]	≤ 0.08	≤ 0.8	≤ 2.0	17-19
Elements	Ni	Ti	S	P
[wt. %]	9-11	5 x C (≤ 0.7)	0.015	0.045

Table 2. Chemical composition of welding wire OK Tigrod 12.60

Elements	**C**	**Si**	**Mn**
[wt. %]	0.1	0.6	1.2

The tests differ from immersion tests mainly in the use of either blasting or pre-tensioning devices themselves; at the same time, no aggressive corrosive solution was used (boric acid is a weak acid), and the significant corrosive medium was, therefore, mostly dissolved oxygen. At the same time, the used medium was circulated through the autoclave. The primary goal is to reveal susceptibility to SCC (in contrast to immersion tests, whose tasks are generally to determine the

resistance of metal materials to corrosion in solutions - sodium chloride solution is most often used).

2.1 The Slow Strain Rate Testing (SSRT)

During the SSRT test, the tensile specimens (L_0 = 25.4 mm and circular cross-section S_0 = 12.56 mm^2) were fixed in the holders of the blasting device (Fig. 1). One specimen was tested during one test – three specimens were used for individual deformation rates. An H_3BO_3 solution with a concentration of 13 g/dm3 was added to the chamber and heated to a temperature of 60°C. After this operation, the SSRT program was started on the PC, where the deformation rates (A:10^{-5}, B:$10^{-6,}$ and C:10^{-7} 1/s) were set.

Fig. 1. Specimen pulled during SSRT

2.2 Exposure in Corrosion Autoclave

An exposure test of the specimens was performed in an autoclave connected to a recirculation loop. The conditions in the autoclave were as follows: the boric acid solution in demi-water had a concentration of 9 g/dm^3 with the addition of KOH (14.3 mg/dm^3). Oxygen, in the range of 7.0 – 7.4 mg/kg, was intentionally added to the solution. Oxygen was added to the reservoir with the solution from the gas cylinder by means of solenoid valves controlled by the control box, and as the amount of oxygen increased, nitrogen was admitted to the solution to remove the excess. Temperature and pressure were set to 270°C and 12.26 N/mm^2. The total number of specimens placed in the autoclave was five with dimensions of approx. 70 x 5 x 1.5 mm (Fig. 2). These were weighed before exposure. Four specimens were inserted into the prestressing devices and were prestressed at the weld metal-base metal (WM-BM) interface by means of screws and ceramic balls by the 3-point bending to the yield strength or 3 % plastic deformation, respectively (based on NACE standard TM0177-2016, method B – Fig. 3). Values of R_e and $\sigma_{3\%}$ were calculated for AISI 321 in 270°C. One specimen was bent at the WM-BM interface to 60°. Subsequently, the specimens were placed in an autoclave, and the test was started while the exposure time was 60 days.

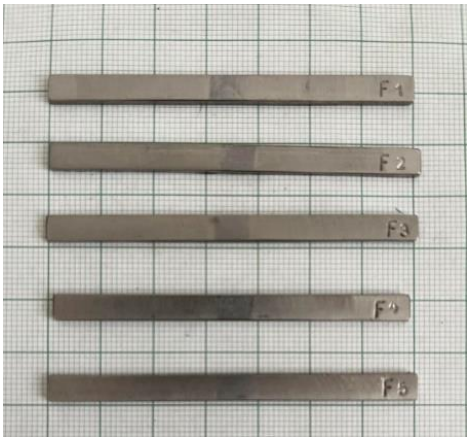

Fig. 2. Specimens for exposition in autoclave

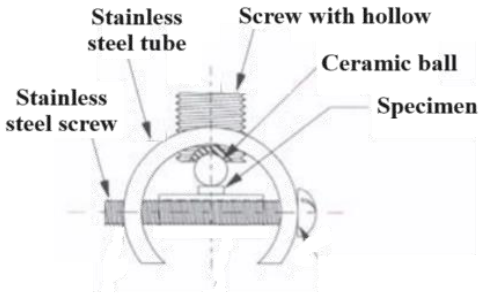

Fig. 3. Diagram of specimen bending (modified diagram from NACE TM0177-2016)

3. RESULTS AND DISCUSSION

After performing both types of tests, the specimens were analysed using stereomicroscopy, light microscopy, confocal microscopy, and SEM. Places of cracks, fractures (SSRT), or pits were observed.

3.1 Results of Slow Strain Rate Testing

The SSRT tests were carried out, where it was found that at the rates of 10^{-5} 1/s (A) and 10^{-6} 1/s (B), a ductile fracture formed in the base metal (tensile fractures). However, using the SEM, cracks were observed at the WM-BM interface in specimen B. They contained a significant amount of corrosion products around their circumference.

Using stereomicroscopy, pits and corrosion products on the surface of the ferritic weld metal were observed on the specimens, as well (Fig. 4).

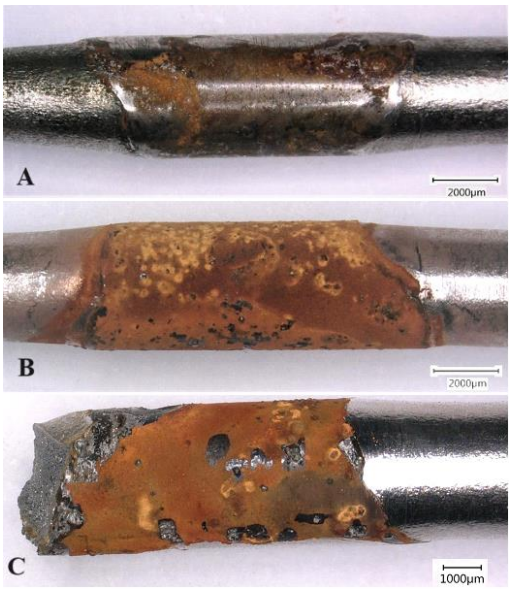

Fig. 4. Weld joints of specimens after SSRT obtained by stereomicroscopy

On the other hand, specimen C, which had a deformation rate of 10^{-7} 1/s, had a fracture at the WM-BM interface, while the marginal part of the fracture contained corrosion products, and thus, it was a ferritic weld metal (the fracture in this place shows brittle behaviour), while the rest of the fracture passed into the austenitic material and has a ductile character. It is, therefore, possible to speak, to a certain extent, of the corrosion cracking or a combination of corrosion cracking and tensile fracture since it was precisely in the austenitic part that it was a tensile ductile fracture (Fig. 5). In the ferritic weld metal, pits appeared in specimens (for example specimen A – Fig. 6), size of which in no case exceeded 50 µm. Fig. 7 shows a built boundary crack in specimen B obtained by light microscopy. Tables 3 and 4 show the parameters and results from the SSRT test, where the values of the strain rate, elongation ΔL, tensile strength Rm, the location where the fracture occurred, and the type of fracture are given. The time to fracture is also shown, where the SSRT test lasted up to 552 h for the C specimen, which means that the weld metal and the interface were most significantly affected by the corrosive medium. As for the type of fracture, in all the cases, it was a ductile tensile fracture, although, in the case of specimen C, the initiation was in the ferritic weld metal and had the character of corrosion cracking. Exposure time played a significant role in cracks' appearance and fractures.

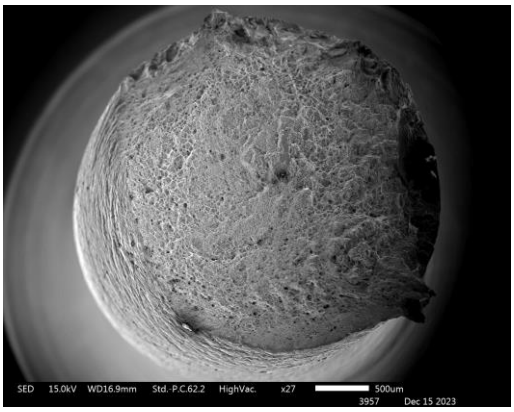

Fig. 5. Fracture surface of specimen C (10^{-7} 1/s) by scanning electron microscope

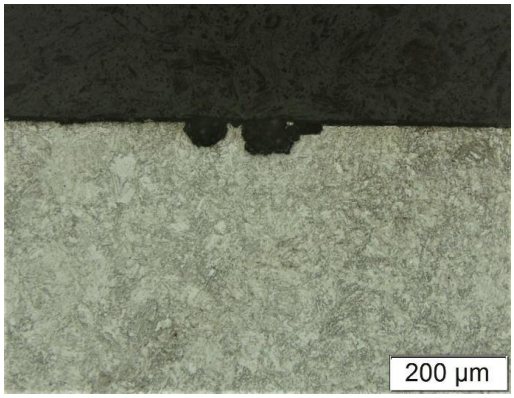

Fig. 6. Pitting on the surface of ferritic weld metal of specimen A (10^{-5} 1/s) obtained by light microscope

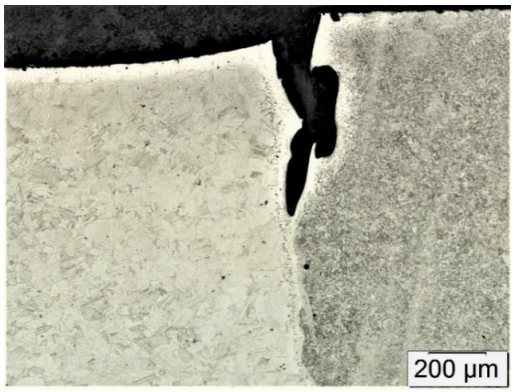

Fig. 7. Crack at the interface weld metal-base metal of specimen B (10^{-6} 1/s) obtained by light microscope

Table 3. Parameters and the results of the SSRT

Sample	**Strain rate** [1/s]	**Time to fracture** [h]	**ΔL** [mm]	**R_m** [N/mm²]
A	10^{-5}	10.3	9.5	579
B	10^{-6}	78.2	7.5	570
C	10^{-7}	552	5.2	548

Table 4. Results of fractures of the SSRT

Sample	Fracture site	Type of fracture
A	5 mm from the interface	ductile
B	7 mm from the interface	ductile
C	interface	ductile with brittle parts

This SSRT test was significantly conservative, and as far as the medium and stress method is concerned, the SSRT had extreme parameters, and in a real primary circuit with real conditions, this type of degradation does not occur. However, it was important to find out how exactly this type of weld metal behaves in more extreme conditions. In this test, the strength of the ferritic region was also confirmed at higher speeds when the tensile fracture occurred, while signs of corrosion cracking began to appear at a strain rate of 10^{-7} 1/s.

3.2 Results of Exposure to Autoclave

The specimens, which were prestressed and exposed in the prepared environment of the H_3BO_3 + KOH solution, were selected after 60 days and observed using a stereomicroscope. The corrosion products of the weld metal were observed (Fig. 8). After the ultrasonic cleaning, the presence of cracks was monitored - but in no case was the presence of cracks confirmed. Specimens were weighed, and the corrosion rates were calculated. Pits were discovered under the corrosion layer in some specimens (F2, F3, and F4), while in specimen F2, which was prestressed to the yield strength, the pits had a maximum depth of 70.6 µm, and in specimens F3 and F4 (prestressed to 3 % plastic deformation), the pits had a maximum depth of 171.2 and 158.1 µm, respectively. Confocal microscopy was used to analyse the depth of the pits (Fig. 9).

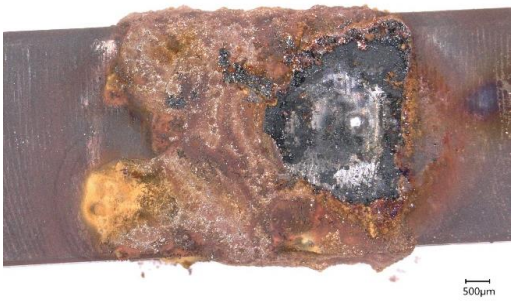

Fig. 8. Weld joint of F4 specimen after exposure in autoclave test

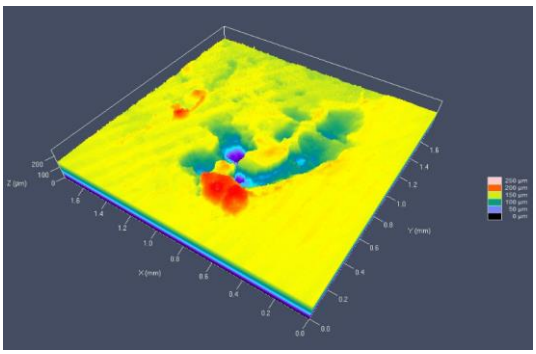

Fig. 9. Analysis of depth of pitting of F4 specimen using confocal microscope

However, specimen F2 had the highest measured corrosion rate (0.21 mm/year), while specimens F3 and F4 had lower corrosion rates of 0.12 and 0.10 mm/year, respectively. Additionally, specimen F1 had a higher corrosion rate. Specimen F5 was not bent precisely at the interface due to the strengthening of the interface region. The buckling occurred close to the interface, and this deformation did not significantly affect the corrosion rate or had the effect on corrosion cracking. The parameters and results of this test are given in Tables 5 and 6. The environment of the prepared solution in the autoclave simulated real conditions in the primary circuits of pressurized water reactors. The only extreme parameter was the artificially added oxygen, whose dissolved amount in the solution was 7.0 to 7.4 mg/kg. Since oxygen is one of the main agents of corrosion in aqueous solutions, its effect on prestressed specimens was monitored. However, despite such extreme levels of dissolved oxygen, no cracks were observed in addition to corrosion products.

Table 5. Parameters of samples preloading

Sample	Level of preloading	$\sigma_{270°C}$ [N/mm^2]	Deflection [mm]
F1	R_e	180	0.52
F2	R_e	180	0.52
F3	$\sigma_{3\%}$	265	0.77
F4	$\sigma_{3\%}$	265	0.77
F5	60° bend	undetermined	-

Table 6. Results of sample exposure

Sample	Area of WM [mm^2]	Corrosion rate [mm/year]	Presence of cracks
F1	101.1	0.13	absent
F2	91.9	0.21	absent
F3	88.4	0.12	absent
F4	92.2	0.10	absent
F5	89.0	0.07	absent

3.3 Discussion

SSRT revealed that at 60°C, ductile fracture occurred in the base material at higher speeds. Similar results but in simulated primary circuit conditions were found by Li and Congleton (also another paper with Charles), who worked with low-alloy steel as weld metal and austenitic steel as base metal, where they found that even at temperatures of 292°C, the test result was that the samples during the SSRT test were tensile tearing in the base material (1-2 mm from interfaces) while the fracture had ductile character, or the fracture occurred at the WM-BM interface as SCC and smoothly transitioned into a strength fracture in the base material [18,19].

In the sample with a slower deformation rate (10^{-7} 1/s), a fracture occurred at the interface, while the initiation started in the ferritic (carbon steel) weld metal, where the fracture had a brittle character and smoothly transitioned to the austenitic part, where the fracture already had a tough character. In many articles, they found that in dissimilar welded joints, SCC often occurs in HAZ or in transition zones [20-22]. Chung et al. [23] analysed the dissimilar type of welds in a combination of low-alloy steel A508 and nickel superalloy 52 and found that with the increasing representation of chromium and nickel in the transition zone, the incidence of SCC decreased during the SSRT test in a simulated primary circuit environment at a temperature of 300°C, a pressure of 10 N/mm^2 and dissolved oxygen with a value of 7 mg/kg. Likewise, with a slower strain rate, the tensile strength also decreased [23]. We also recorded this result in our research. Huang et al. found that the stress corrosion cracking susceptibility of 316LN austenitic steel in a simulated primary water environment decreased with an increasing strain rate and experiment temperature [24].

The articles also mention that transformable ferritic steels are potentially susceptible to hydrogen-induced stress corrosion cracking in a range of environmental conditions, the hydrogen being formed by a cathodic corrosion reaction. It is also generally known that hydrogen embrittlement in most steels occurs sporadically above a temperature of 150°C. On the other hand, austenitic steels have a higher hydrogen embrittlement resistance [22,25-29]. It is very likely that hydrogen diffused into the interface (into the ferritic weld metal part) in sample C, since the strength of carbon steel itself is better than that of austenitic base metal, and the interface itself was strengthened. The hydrogen caused the embrittlement of the ferritic part, and subsequently, a fracture occurred in the austenite.

Exposure of the samples in the autoclave while simulating the primary circuit did not achieve the formation of SCC. Spots of pitting in the weld metal and interface were discovered. Similar results were achieved by Sinjlawi et al. [30], who tested samples of AISI 304 and 316L austenitic steels in the form of plates, which were bent with a bending device to 2-3% plastic deformation while monitoring susceptibility to crevice corrosion and SCC. Under the conditions of a temperature of 325°C, pressure of 15.5 MPa dissolved oxygen (8 mg/kg), and dissolved hydrogen (2.65 mg/kg), the samples were stored in an autoclave for 1000 h. After exposure, the AISI 304 samples contained cracks, while the AISI 316 samples had no cracks. It also had excellent resistance to the significant presence of hydrogen [30]. Other tests were also performed by Raquet et al. [31], who used constant load test and constant deformation test using U-bend samples and 4-point bending (4 and 10% plastic deformation) cold-worked samples in primary water at a temperature of 360°C and exposure time from 4000 to 17000 h found that there was no promotion of SCC in any of the samples. In another article, Hodač and Veselý [32] analysed weld joints made of austenitic steel AISI 321 and low-alloy steel where samples were exposed in boiler water for 53 days. Metallography showed an undamaged weld joint in the specimen which was exposed to demineralised water, but pitting corrosive damage was found on the ferritic side with a maximum depth of 61 µm in the sample exposed in solution of NH_3, N_2H_4, and ions as SO_4^{2-}, Cl^-, F^-, Na^+ (in this sample also austenitic side hade pits with maximum depth of 35 µm – due to Cl^- ions). Also, the average weight loss was increased with the NaCl concentration increased [32].

More research is also focused on the simulation of corrosion cracking using simulating software [5,33,34], while our next possible research could go in this direction as well.

A comparison of SSRT and autoclave exposure showed that even at 60°C and atmospheric pressure, and at 270°C and 12.26 N/mm^2 pressure, the heterogeneous weld joint was relatively resistant to corrosion cracking. The problem with sample C was probably caused by hydrogen embrittlement, which can occur at a temperature of 60°C. The high content of oxygen in the solution in the autoclave caused pitting in the samples. Also,

in the SSRT samples, pitting was observed in the ferritic weld metal and at its interface, which could be caused by the oxygen present (highly demineralized water was used, and therefore, the presence of chlorides was extremely low).

4. CONCLUSIONS

Stress corrosion cracking of heterogeneous weld joints under the conditions of the primary circuit was the main topic of this work, while this area of materials is still not completely clarified since, in SCC, various factors are considered, which can synergistically affect the entire course of this corrosion damage. There is also great interest in the possibility of using other cheaper materials (such as low-alloyed carbon steels) in the primary circuit rather than only austenitic stainless steels or nickel alloys, for example, in welds.

Based on the performed experiments, the following conclusions were drawn about the slow strain rate testing:

- Ductile fractures occurred in specimens with deformation rates of 10^{-5} and 10^{-6} 1/s in the base metal, at a distance of 5 or 7 mm, respectively, from the weld metal-base metal interface.
- The specimen with a deformation rate of 10^{-7} 1/s was broken at the interface, but the initiation of the fracture started in the ferritic weld metal and continued through the austenitic base metal, where the fracture had a ductile character over almost the entire surface, i.e., the fracture itself continued as a typical tensile fracture and not as a corrosion fracture.

The exposure in the autoclave tests:

- The analysis did not show the formation of cracks in the weld metal at the WM-BM interface or in any part of the exposed specimens.
- Future research would focus on the combination of SSRT with electrochemical measurements at a temperature of 60°C (open circuit potential - OCP measurement), which would more perfectly describe the events during this test. At the same time, samples in the form of tensile samples at SSRT with the same parameters could be used in the autoclave. Here, as in the cited articles, other methods of mechanical loading could be used, either a cyclic test or a constant load test.

ACKNOWLEDGEMENT

This work was supported by the Slovak Research and Development Agency under the Contract no. APVV-22-0146. Thanks are due to Research Welding Institute, especially Research and Development Division of Welding Technologies and Equipment, for helping with experiments and data evaluation.

Conflicts of Interest

The authors declare no conflict of interest.

REFERENCES

[1] O. Matal, H. Šen, Nuclear facilities and their safety. *University of Technology*, Brno, 2016.

[2] P. Pedeferri, Corrosion Science and Engineering. *Springer*, Milan, 2018.

[3] M. Wang, L. Chen, X. Liu, X. Ma, Influence of thermal aging on the SCC susceptibility of wrought 316LN stainless steel in a high temperature water environment. *Corrosion Science*, 81, 2014: 1488-1518. https://doi.org/10.1016/j.corsci.2013.12.011

[4] D. Tice, Contribution of research to the understanding and mitigation of environmentally assisted cracking in structural components of light water reactors. *Corrosion Engineering, Science and Technology*, 53(1), 2017: 11-25. https://doi.org/10.1080/1478422X.2017.1362158

[5] Y. Sun, H. Xue, K. Zhao, Y. Zhang, Y. Zhao, W. Yan, R. Bashir, Cracking Driving Force at the Tip of SCC under Heterogeneous Material Mechanics Model of Safe-End Dissimilar Metal-Welded Joints in PWR. *Science and Technology of Nuclear Installations*, 2022, 2022: 1-10. https://doi.org/10.1155/2022/6605101

[6] S. Lozano-Perez, J. Dohr, M. Meisnar, K. Kruska, SCC in PWRs: Learning from a Bottom-Up Approach. *Metallurgical and Materials Transactions E*, 1, 2014: 194-210. https://doi.org/10.1007/s40553-014-0020-y

[7] D.A. Jones, Principles and prevention of corrosion. *Prentice Hall*, New Jersey, 1996.

[8] L. Dong, Q. Peng, E.-H. Han, W. Ke, L. Wang, Stress corrosion cracking in the heat affected zone of a stainless steel 308L-316L weld joint in primary water. *Corrosion Science*, 107, 2016: 172-181. https://doi.org/10.1016/j.corsci.2016.02.030

[9] H.J. Qu, J.P. Wharry, Nanoindentation Investigation of Chloride-Induced Stress Corrosion Crack Propagation is an Austenitic Stainless Steel Weld. *Metals*, 12(8), 2022: 1243. https://doi.org/10.3390/met12081243

[10] S. Weng, Y. Huang, F. Xuan, F. Yang, Pit evolution around the fusion line of a NiCrMoV steel welded joint caused by galvanic and stress-assisted coupling corrosion. *RSC Advances*, 8, 2018: 3399-3409. https://doi.org/10.1039/C7RA11837F

[11] K.Q. Zhang, Z.M. Tang, S.L. Hu, P.Z. Zhang, Effect of cold work and slow strain rate on 321SS stress corrosion cracking in abnormal conditions of simulated PWR primary environment. *Nuclear Materials and Energy*, 20, 2019: 1-6. https://doi.org/10.1016/j.nme.2019.100697

[12] Z. Shen, D. Du, L. Zhang, S. Lozano-Perez, An insight into PWR primary water SCC machanisms by comparing surface and crack oxidation. *Corrosion Science*, 148, 2019: 213-227. https://doi.org/10.1016/j.corsci.2018.12.020

[13] D.L. Olson, A.N. Lasseigne, M. Marya, B. Mishra, G. Castro, Materials Science Aspects of Weld Corrosion. *Proc. of International Conference on Welding and Joining of Materials*, 27-29 October 2003, Lima, Peru.

[14] M. Henthorne, The Slow Strain Rate Stress Corrosion Cracking Test – A 50 Year Retrospective. *Corrosion*, 72(12), 2016: 1488-1518. https://doi.org/10.5006/2137

[15] E.A. Krivonosova, A Review of Stress Corrosion Cracking of Welded Stainless Steels. *Open Access Library Journal*, 5, 2018: e4568. https://doi.org/10.4236/oalib.1104568

[16] A. Guzanová, J. Brezinová, J. Viňáš, J. Koncz, Determination of the corrosion rate of weld joints realized by MAG technology. *KOM - Corrosion and Material Protection*, 61(1), 2017: 19-24. https://doi.org/10.1515/kom-2017-0002

[17] B.N. Popov, J.-W. Lee, M.B. Djukic, Chapter 7 - Hydrogen Permeation and Hydrogen-Induced Cracking. Handbook of Environmental Degradation of Materials (Third Edition). *William Andrew Publishing*, 2018. https://doi.org/10.1016/B978-0-323-52472-8.00007-1

[18] G.F. Li, J. Congleton, Stress corrosion cracking of low alloy steel to stainless steel transition weld in PWR primary waters at 292°C. *Corrosion Science*, 42(6), 2000: 1005-1021. https://doi.org/10.1016/S0010-938X(99)00131-6

[19] G.F. Li, E.A. Charles, J. Congleton, Effect of post weld heat treatment on stress corrosion cracking of a low alloy steel to stainless steel transition weld. *Corrosion Science*, 43(10), 2001: 1963-1983. https://doi.org/10.1016/S0010-938X(00)00182-7

[20] M. Ragavendran, A. Toppo, M. Vasudevan, SCC behaviour of laser and hybrid laser welded stainless steel weld joints. *Materials Science and Technology*, 38(5), 2022: 281-298. https://doi.org/10.1080/02670836.2022.2043027

[21] J. Labanowski, Stress corrosion cracking susceptibility of dissimilar stainless steels welded joints. *Journal of Achievements in Materials and Manufacturing Engineering*, 20(1-2), 2007: 255-258.

[22] J.R. Davis, Corrosion of Weldments. *ASM International*, Cleveland, 2006.

[23] W.-C. Chung, J.-Y. Huang, L.-W. Tsay, C. Chen, Microstructure and Stress Corrosion Cracking Behavior of the Weld Metal in Alloy 52-A508 Dissimilar Welds. *Materials Transactions*, 52(1), 2011: 12-19. https://doi.org/10.2320/matertrans.M2010294

[24] Y. Huang, W. Wu, S. Cong, G. Ran, D. Cen, N. Li, Stress Corrosion Behaviors of 316LN Stainless Steel in a Simulated PWR Primary Water Environment. *Materials*, 11(9), 2018: 1509. https://doi.org/10.3390%2Fma11091509

[25] T.G. Gooch, Stress Corrosion Cracking of Ferritic Steel Weld Metal – the Effect of Nickel. *Metal Construction,* 14(1), 1982: 29-33.

[26] H. Husby, P. Wagstaff, M. Iannuzzi, R. Johnsen, M. Kappes, Effect of Nickel on the Hydrogen Stress Cracking Resistance of Ferritic/Pearlitic Low Alloy Steels. *Corrosion*, 74(7), 2018: 801-818. http://dx.doi.org/10.5006/2724

[27] A. Contreras, M. Salazar, A. Albiter, R. Galván, O. Vega, Arc Welding: Assessment of Stress Corrosion Cracking on Pipeline Steels Weldments Used in the Petroleum Industry by Slow Strain Rate Tests. *InTech*, 2011. http://dx.doi.org/10.5772/26569

[28] H. Park, C. Park, J. Lee, H. Nam, B. Moon, Y. Moon, N. Kang, Microstructural aspects of hydrogen stress cracking in seawater for low carbon steel welds produced by flux-cored arc

welding. *Materials Science & Engineering*, 820, 2021: 141568. https://doi.org/10.1016/j.msea.2021.141568

[29] J. Liu, M. Zhao, L. Rong, Overview of hydrogen-resistant alloys for high-pressure hydrogen environment: on the hydrogen energy structural materials. *Clean Energy*, 7(1), 2023: 99-115. https://doi.org/10.1093/ce/zkad009

[30] A. Sinjlawi, J. Chen, H.-S. Kim, H. B. Lee, C. Jang, S. Lee, Role of residual ferrites on crevice SCC of austenitic stainless steels in PWR water with high-dissolved oxygen. *Nuclear Engineering and Technology*, 52(11), 2020: 2552-2564. https://doi.org/10.1016/j.net.2020.04.023

[31] O. Raquet, E. Herms, F. Vaillant, T. Couvant, J.M. Boursier, 6 - Effect of cold work hardening on stress corrosion cracking of stainless steels in primary water of pressurized water reactors. Corrosion Issues in Light Water Reactor. *Woodhead Publishing,* 2007: 76-86. https://doi.org/10.1533/9781845693466.2.76

[32] J. Hodač, V. Veselý, Dissimilar weld joint corrosion in simulated boiler water environment. *KOM – Corrosion and Material Protection Journal*, 66(1), 2022: 16-19. https://doi.org/10.2478/kom-2022-0003

[33] G.B. Li, H. Xue, Y.Q. Bi, L. Zhang, Study on the Rate of Elastic-plastic Crack Propagation of Heterogeneous Metal Welded Joints in Nuclear Power. *IOP Conference Series: Materials Science and Engineering*, 751, 2020: 012063. https://doi.org/10.1088/1757-899X/751/1/012063

[34] Y. Zhang, H. Xue, S. Zhang, S. Wang, Y. Sun, Y. Zhang, Y. Yang, Interaction of Mechanical Heterogeneity and Residual Stress on Mechanical Field at Crack Tips in DMWJs. *Science and Technology of Nuclear Installations*, 2022, 2022: 7462200. https://doi.org/10.1155/2022/7462200